Nonlinear optical dynamics of 2D super-crystals of quantum Λ-emitters

Igor V. Ryzhov[1], Ramil F. Malikov[2], Andrey V. Malyshev[3,4], Victor A. Malyshev[1,5]

[1]Herzen State Pedagogical University, St. Petersburg, 191186 Russia
[2]M. Akmullah Bashkir State Pedagogical University, 450008 Ufa, Russia
[3]GISC, Física de Materiales, Universidad Complutense, E-28040 Madrid, Spain
[4]Ioffe Physical-Technical Institute, 26 Politechnicheskaya str., 194021 St.-Petersburg, Russia
[5]Zernike Institute for Advanced Materials, University of Groningen, Nijenborgh 4, 9747 AG Groningen, The Netherlands

E-mail: a.malyshev@fis.ucm.es

E-mail: igoryzhov@yandex.ru

Abstract. We study theoretically the optical response of a 2D super-crystal of quantum Λ-emitters which are coupled by their secondary dipole field. The latter introduces a feedback into the system, the interplay of which with the intrinsic nonlinearity of emitters results in an exotic behavior of the system's optical response, such as periodic or quasi-periodic self-oscillations and chaotic dynamics. We argue therefore that these predicted features can be promising for various nanophotonic applications.

1. Introduction

Metasurfaces comprising (meta)atoms have been thoroughly investigated recently due to their possible remarkable applications in the domain of light manipulation and sub-wavelength nanophotonics [1, 2, 3]. For example, atomically thin layer of $MoSe_2$ encapsulated in hexagonal BN manifests high reflectance in the vicinity of collective (excitonic) resonance [4, 5]. Arrays of atoms trapped in an optical lattice [6] and two-dimensional supercrystals of semiconductor quantum dots (SQDs) [7, 8, 9] exhibit similar behavior. It was demonstrated also that the optical response of the SQD super-crystals can demonstrate multistability and instabilities of different types, including periodic and aperiodic self-oscillations and chaotic dynamics [10, 11].

In this contribution, we are modelling the reflection of the quasi-resonant radiation from a monolayer of quantum emitters with the Λ-type arrangement of the energy levels. The secondary field of all other emitter acting on a given one provides a feedback which, combined with the intrinsic nonlinearity of the emitter itself, can result in a very rich optical dynamics. The latter can manifest itself in various types of instabilities of measurable quantities such as the reflectance.

2. Model and formalism

Our model system is an $N \times N$ square lattice of identical quantum emitters having a single upper state $|3\rangle$ and a doublet $|1\rangle$ and $|2\rangle$ in the lower state. The doublet splitting Δ_{21} is assumed to be

Content from this work may be used under the terms of the Creative Commons Attribution 3.0 licence. Any further distribution of this work must maintain attribution to the author(s) and the title of the work, journal citation and DOI.
Published under licence by IOP Publishing Ltd

small compared to the optical transition frequencies ω_{31} and ω_{32}. Optical transitions are allowed only between the upper state $|3\rangle$ and those of the doublet $|1\rangle$ and $|2\rangle$ (the so-called Λ-scheme); they are characterized by their transition dipole moments $\mathbf{d_{31}}$ and $\mathbf{d_{32}}$ which are taken to be real and parallel to each other, for the sake of simplicity: $\mathbf{d}_{32} = \mu\mathbf{d_{31}}$. The spontaneous decay of the upper state $|3\rangle$ to the doublet states $|2\rangle$ and $|1\rangle$ is characterized by the rates γ_{31} and $\gamma_{32} = \mu^2\gamma_{31}$, respectively. The rate γ_{21} characterises the relaxation within the doublet. The system is excited by the quasi-resonant continuous wave (CW) external field $\boldsymbol{\mathcal{E}} = \mathbf{E}_0\cos(\omega_0 t)$ at normal incidence; the field is polarized along the transition dipole moments. All emitters interact with each other via their secondary retarded dipole field which includes the near- and far-zone contributions. Hereafter, we use the mean-field approximation in which the secondary field does not depend on the position of the emitter.

Within the rotating wave approximation, the optical dynamics of the "mean" Λ-emitter is governed by the following system of equations for the density matrix $\rho_{\alpha\beta}$ $(\alpha, \beta = 1, 2, 3)$:

$$\dot{\rho}_{11} = \gamma_{21}\rho_{22} + \gamma_{31}\rho_{33} + \Omega^*\rho_{31} + \Omega\rho_{31}^* \tag{1a}$$
$$\dot{\rho}_{22} = -\gamma_{21}\rho_{22} + \gamma_{32}\rho_{33} + \mu(\Omega^*\rho_{32} + \Omega\rho_{32}^*) \tag{1b}$$
$$\dot{\rho}_{33} = -(\gamma_{31} + \gamma_{32})\rho_{33} - \Omega^*\rho_{31} - \Omega\rho_{31}^* - \mu(\Omega^*\rho_{32} + \Omega\rho_{32}^*) \tag{1c}$$
$$\dot{\rho}_{31} = -\left[i\Delta_{31} + (\gamma_{31} + \gamma_{32})/2 + \Gamma\right]\rho_{31} + \Omega(\rho_{33} - \rho_{11}) - \mu\Omega\rho_{21} \tag{1d}$$
$$\dot{\rho}_{32} = -\left[i\Delta_{32} + (\gamma_{31} + \gamma_{32} + \gamma_{21})/2 + \Gamma\right]\rho_{32} + \mu\Omega(\rho_{33} - \rho_{22}) - \Omega\rho_{21}^* \tag{1e}$$
$$\dot{\rho}_{21} = -\left(i\Delta_{21} + \gamma_{21}/2\right)\rho_{21} + \mu\Omega^*\rho_{31} + \Omega\rho_{32}^* \,, \tag{1f}$$

$$\Omega = \Omega_0 + (\gamma_R - i\Delta_L)(\rho_{31} + \mu\rho_{32}) \,, \tag{2}$$

where $\Delta_{31} = \omega_0 - \omega_{31}$ and $\Delta_{32} = \omega_0 - \omega_{32}$ are detunings of the incident field frequency ω_0 from the resonance frequencies ω_{31} and ω_{32} of the $1 \leftrightarrow 3$ and $2 \leftrightarrow 3$ transitions, respectively, and Γ is the dephasing rate (it is taken to be the same for both transitions for the sake of simplicity). The Rabi amplitude of the total field with the amplitude E is $\Omega = d_{31}E/\hbar$ ($\hbar$ is the reduced Plank constant) and it is given by Eq. 2. The first term in Eq. 2, $\Omega_0 = d_{31}E_0/\hbar$ stands for the Rabi amplitude of the incident field with the amplitude E_0 while the second term is the Rabi amplitude of the secondary field produced by all other emitters at the position of a given one. The part proportional to γ_R describes the far-zone contribution of the secondary field; it is the Dicke superradiant constant [12, 13, 14, 10] determining the collective radiation relaxation rate of Λ-emitters in the monolayer. On the other hand, the part proportional to Δ_L accounts for the near-zone contribution; it is analogous to the Lorentz local field [15] and determines the (excitonic) energy level renormalization [15, 10, 16]. Irrespective of the system size, $\Delta_L \gg \gamma_R$ for a dense sample ($\lambda \gg a$). Finally, we note that Eqs. (1a-1f) conserve the total population: $\rho_{11} + \rho_{22} + \rho_{33} = 1$, i. e. we consider the spontaneous decay to be the only channel of the population relaxation.

In what follows, we address the system reflectance R (the reflection coefficient of the energy flow) defined as

$$R = \left|\frac{\Omega_{\text{refl}}}{\Omega_0}\right|^2 \,, \quad \Omega_{\text{refl}} = \gamma_R(\rho_{31} + \mu\rho_{32}) \,, \tag{3}$$

where Ω_{refl} is the Rabi amplitude of the reflected field.

3. Results

In our calculations we use the set of parameters typical for 2D supercrystals of SQDs [7, 10]: $\gamma_{31} = \gamma_{32} \approx 3 \cdot 10^9$ s^{-1} ($\mu = 1$ for simplicity), then for $\lambda \sim 100 \div 200$ nm and $a \sim 10 \div 20$ nm, $\gamma_R \sim 10^{12}$ s^{-1} and $\Delta_L \sim 10^{13}$ s^{-1}. We set therefore $\gamma_R = 100\gamma_{31}$ and $\Delta_L = 1000\gamma_{31}$. In what follows, we present our results calculated for $\Delta_{31} = 1000$, $\Delta_{21} = 100$, $\gamma_{21} = 0.01$ and

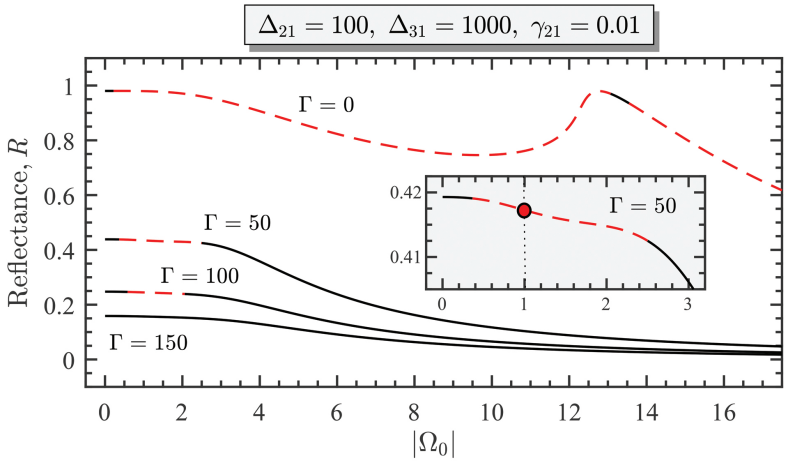

Figure 1. Steady-state reflectance R as a function of the Rabi magnitude $|\Omega_0|$ of the incident field, calculated for different values of the dephasing rate Γ indicated in the plot. Stable and unstable parts of the curves are given by solid black and dashed red lines, respectively. The inset blows up the reflectance curve calculated for $\Gamma = 50$ in the vicinity of $|\Omega_0| = 1$.

different values of the dephasing rate Γ. The spontaneous emission rate γ_{31} is used as the unit of frequency and γ_{31}^{-1} as the time unit.

First, we address the steady-state reflectance R as a function of the Rabi magnitude of the incident field $|\Omega_0|$ calculated for different values of the dephasing rate Γ. We use the standard local Lyapunov exponent analysis to determine the stability of the steady-state reflectance. The results are presented in Fig. 2 which shows that a region of unstable solutions (given by the red dashed line) exists for relatively low values of $|\Omega_0|$, which is both surprising and promising for the experiment. As can be seen from the figure, the region of instabilities shrinks as the dephasing rate Γ increases, as expected. As the unstable regions shrink, more complex dynamical regimes, such as quasi-periodic oscillations and chaos, predicted for $\Gamma = 0$ in Ref. [16] (not shown here), disappear. A detailed study of the bifurcation diagram of the system will be addressed elsewhere. In what follows, we restrict ourselves to a simple periodic self-oscillation regime.

To analyse the character of the reflectance instability, we calculated the system dynamics for a relatively high value of the dephasing rate, $\Gamma = 50$, and a relatively low value of the Rabi magnitude of the incident field, $|\Omega_0| = 1$, which falls within the unstable region of R (see the vertical dotted line in the inset of Fig. 1). The calculation was made for the ground state initial condition. Eqs. (1a–1f) were integrated until all transients vanished and the system converged to an attractor. Then, the Fourier magnitude spectrum $|\int \Omega_{\rm refl}(t) \exp(i\omega t) dt|$ and the phase space map $(\mathrm{Re}[\Omega_{\rm refl}(t)], \mathrm{Im}[\Omega_{\rm refl}(t)])$ of the attractor trajectory was calculated. The results are presented in Fig. 2 which shows that the system converges to the attractor with a periodic self-oscillations: the attractor trajectory is a closed line in the phase space and its Fourier spectrum is a finite set of equidistant lines. Note that the frequencies of the self-oscillation fall into the THz domain and that the reflectance oscillates in the range $\approx (0.2, 0.4)$. Bearing also in mind that the excitation power density corresponding to $|\Omega_0| = 1$ is attainable in experiment, we argue that such a self-oscillation of the reflectance is presumably measurable.

4. Conclusions

In conclusion, we studied theoretically the steady state and the dynamics of the reflectance of a 2D metasurface comprizing regularly spaced quantum Λ-emitters subjected to a CW quasi-resonant excitation. Using the Lyapunov exponent analysis we showed that the steady state

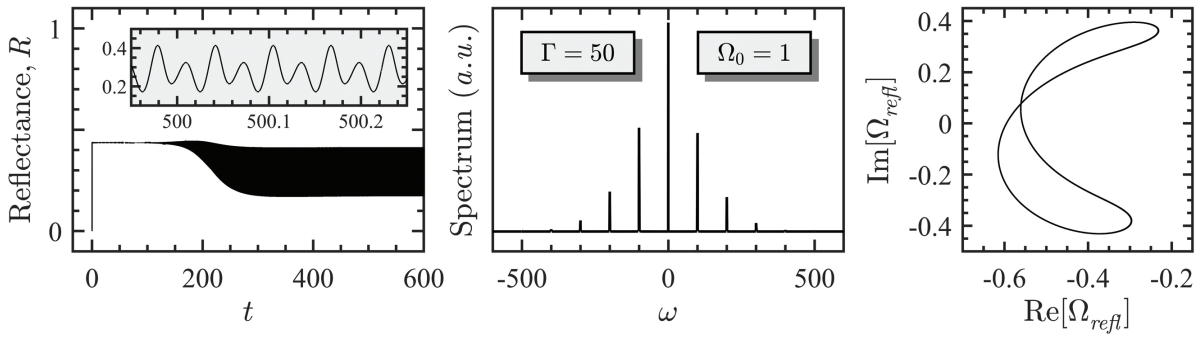

Figure 2. Dynamics of the reflectance R (left panel) calculated for $\Gamma = 50$ and $|\Omega_0| = 1$; the inset blows up the self-oscillatory dynamics on the attractor. Characteristics of the attractor: the Fourier magnitude spectrum (central panel) and the phase space map (right panel).

has regions of unstable solutions. Our analysis of the system dynamics demonstrates that the system can be in a periodic self-oscillation regime even for relatively strong dephasing rate and low excitation power densities ($\lesssim 1\mathrm{W/cm}^2$). We argue therefore that the predicted effect can probably be measured experimentally. We note also that the frequency of these THz self-oscillations depend on the intensity of the excitation field, making them tunable. We argue therefore that our results suggest various practical applications of metasurfases of quantum Λ-emitters, in particular, a tunable generator of coherent THz radiation, which makes the system a promising building block for nanophotonics devices.

Acknowledgements
R. F. M. acknowledges financial support from M. Akmullah Bashkir State Pedagogical University. A. V. M. acknowledges support from Spanish MICIN grants MAT2016-75955 and PID2019-106820RB-C21.

References

[1] Chen H T, Taylor A J and Yu N 2016 *Rep. Progr. Phys.* **79** 076401
[2] Hsiao H H, Chu C H and Tsai D P 2017 *Small Methods* **1** 1600064
[3] Chang S, Guo X and Ni X 2018 *Annual Review of Materials Research* **48** 279–302
[4] Back P, Zeytinoglu S, Ijaz A, Kroner M and Imamoğlu A 2018 *Phys. Rev. Lett.* **120**(3) 037401
[5] Scuri G, Zhou Y, High A A, Wild D S, Shu C, De Greve K, Jauregui L A, Taniguchi T, Watanabe K, Kim P, Lukin M D and Park H 2018 *Phys. Rev. Lett.* **120**(3) 037402
[6] Bekenstein R, Pikovski I, Pichler H, Shahmoon E, Yelin S F and Lukin M D 2020 *Nat. Physics* **16** 676
[7] Evers W H, Goris B, Bals S, Casavola M, de Graaf J, van Roij R, Dijkstra M and Vanmaekelbergh D 2013 *Nano Lett.* **13** 2317
[8] Baimuratov A S, Rukhlenko I D, Turkov V K, Baranov A V and Fedorov A V 2013 *Sci. Rep.* **3** 1727
[9] Baimuratov A S, Shlykov A I, Zhu W, Leonov M Y, Baranov A V, Fedorov A V and Rukhlenko I D 2017 *Opt. Lett.* **42** 2423
[10] Ryzhov I V, Malikov R F, Malyshev A V and Malyshev V A 2019 *Phys. Rev. A* **100** 003800
[11] Bayramdurdiyev D Y, Malikov R F, Ryzhov I V and Malyshev V A 2020 *J. Exp. Theor. Phys.* **131** 244
[12] Dicke R H 1954 *Phys. Rev.* **93** 99
[13] Trifonov E D, Zaitsev A I and Malikov R F 1979 *Sov. Phys. JETP* **49** 33
[14] Benedict M G, Ermolaev A M, Malyshev V A, Sokolov I V and Trifonov E D 1996 *Super-radiance: Multiatomic Coherent Emission* (IOP Publishing, Bristol)
[15] Benedict M G, Zaitsev A I, Malyshev V A and Trifonov E D 1991 *Phys. Rev. A* **43** 3845
[16] Ryzhov I V, Malikov R F, Malyshev A V and Malyshev V A 2021 *J. Opt.* https://doi.org/10.1088/2040–8986/ac2788